

RESEARCH ARTICLE

Open Access



The novel roles of YULINK in the migration, proliferation and glycolysis of pulmonary arterial smooth muscle cells: implications for pulmonary arterial hypertension

Yi-Chia Wu^{1,2,3,4}, Wei-Ting Wang¹, Ming-Chun Yang^{5,6}, Yu-Tsun Su^{5,6}, Jwu-Lai Yeh⁷, Jong-Hau Hsu^{8,9} and Jiunn-Ren Wu^{5*} 

Abstract

Background Abnormal remodeling of the pulmonary vasculature, characterized by the proliferation and migration of pulmonary arterial smooth muscle cells (PASMCs) along with dysregulated glycolysis, is a pathognomonic feature of pulmonary arterial hypertension (PAH). *YULINK* (MIOS, Entrez Gene: 54468), a newly identified gene, has been recently shown to possess pleiotropic physiologic functions. This study aims to determine novel roles of YULINK in the regulation of PAH-related pathogenesis, including PASMC migration, proliferation and glycolysis.

Results Our results utilized two PAH-related cell models: PASMCs treated with platelet-derived growth factor (PDGF) and PASMCs harvested from monocrotaline (MCT)-induced PAH rats (PAH-PASMCs). *YULINK* modulation, either by knockdown or overexpression, was found to influence PASMC migration and proliferation in both models. Additionally, YULINK was implicated in glycolytic processes, impacting glucose uptake, glucose transporter 1 (GLUT1) expression, hexokinase II (HK-2) expression, and pyruvate production in PASMCs. Notably, YULINK and GLUT1 were observed to colocalize on PASMC membranes under PAH-related pathogenic conditions. Indeed, increased YULINK expression was also detected in the pulmonary artery of human PAH specimen. Furthermore, YULINK inhibition led to the suppression of platelet-derived growth factor receptor (PDGFR) and the phosphorylation of focal adhesion kinase (FAK), phosphoinositide 3-kinase (PI3K), and protein kinase B (AKT) in both cell models. These findings suggest that the effects of YULINK are potentially mediated through the PI3K-AKT signaling pathway.

Conclusions Our findings indicate that YULINK appears to play a crucial role in the migration, proliferation, and glycolysis in PASMCs and therefore positioning it as a novel promising therapeutic target for PAH.

Keywords YULINK, Pulmonary arterial hypertension (PAH), Pulmonary arterial smooth muscle cells (PASMCs), Migration, Proliferation, Glycolysis

*Correspondence:

Jiunn-Ren Wu
jirewu@gmail.com

Full list of author information is available at the end of the article



© The Author(s) 2023. **Open Access** This article is licensed under a Creative Commons Attribution 4.0 International License, which permits use, sharing, adaptation, distribution and reproduction in any medium or format, as long as you give appropriate credit to the original author(s) and the source, provide a link to the Creative Commons licence, and indicate if changes were made. The images or other third party material in this article are included in the article's Creative Commons licence, unless indicated otherwise in a credit line to the material. If material is not included in the article's Creative Commons licence and your intended use is not permitted by statutory regulation or exceeds the permitted use, you will need to obtain permission directly from the copyright holder. To view a copy of this licence, visit <http://creativecommons.org/licenses/by/4.0/>. The Creative Commons Public Domain Dedication waiver (<http://creativecommons.org/publicdomain/zero/1.0/>) applies to the data made available in this article, unless otherwise stated in a credit line to the data.

Background

Pulmonary arterial hypertension (PAH) is an unusual but life-threatening disease characterized by increases in pulmonary vascular resistance (PVR), which eventually leads to right ventricular (RV) failure and death [1]. In the 6th World Symposium on Pulmonary Hypertension in Nice, France (2018), one of the new definitions of PAH was redefined as a mean pulmonary artery pressure (mPAP) > 20 mmHg, pulmonary arterial wedge pressure > 15 mmHg, plus pulmonary vascular resistance index > 3 Wood units/m² [2]. The estimated prevalence of PAH was reported to be 26–33 cases per million in the US and 20–40 cases per million in Europe [3].

In PAH, continuously elevated mPAP has been demonstrated to correlate with the reconstruction and remodeling of pulmonary vascular structure characterized by an accumulation of different vascular cells in endothelial proliferation and hyperplasia of the medial muscular layer and collagen-rich fibrosis of adventitia. Excessive pulmonary artery smooth muscle cell (PASMC) proliferation and migration resulting in pulmonary arterial wall thickening is the most conspicuous feature in the pathological development of PAH [4]. Among these factors, platelet-derived growth factor (PDGF) has been widely recognized as a key regulator that triggers uncontrolled and dysregulated migration and proliferation of PASMCs in PAH pathogenesis [5].

In addition to the pathophysiological hyperproliferation and cell migration of PASMCs, a cancer-like abnormal metabolic phenotype named the “Warburg effect” has been clarified in PAH [6]. In this metabolic abnormality, the cells tend to favor an anaerobic respiration pathway with upregulated glycolysis over defective mitochondrial respiration, and furthermore, PDGF-triggered PASMC proliferation is evidenced as accompanying higher glucose consumption and lactose production. Treatment with PDGF stimulates a constitutive increase in glucose transporters and the expression of the glycolysis marker GLUT1 [7, 8]. Upregulated glycolytic gene expression was also found in hyperproliferative pulmonary artery fibroblasts isolated from PAH patients [9]; therefore, targeting PDGF-related signaling pathways has been considered an attractive strategy in PAH therapeutics.

According to comparative evolutionary genomics analysis, we previously identified a gene named *YULINK* (*MIOS*, Entrez Gene: 54468) that is evolutionarily conserved from zebrafish to humans and encodes an 875 amino acid protein containing WD40 repeats at the N-terminus in humans [10]. Deficiency of *YULINK* resulted in irregular Ca²⁺ cycling and contributed to the induction of cardiac arrhythmia in both mouse and human models [10]. *YULINK* contains a highly

conserved domain, *MIOS* (missing oocyte, gene ID: 33399), which was revealed to participate in the regulation of mTOR signaling [11]. mTOR signaling plays critical roles in cell migration, cell proliferation and energy homeostasis in PASMCs in PAH [12]; however, whether *YULINK* participates in PAH-related pathophysiological abnormalities, especially in cell migration, proliferation and glycolytic function, has not yet been investigated.

In this study, the role of *YULINK* in cell migration, proliferation and glycolysis in PASMCs treated with PDGF or PASMCs derived from rats with MCT-induced PAH was examined, and the results indicated that the level of *YULINK* expression was correlated with cell migration and proliferation in PASMCs treated with PDGF or PASMCs derived from rats with MCT-induced PAH (PAH-PASMCs). Glucose uptake and glycolysis in PASMCs could be regulated by *YULINK* through GLUT1 interaction. *YULINK* suppression inhibited cell migration, proliferation, and glycolysis in PAH cell models, which could be mediated through the PI3K-AKT signaling pathways. These findings provide a possible mechanistic link between *YULINK* and the pathogenesis of PAH.

Materials and methods

Animals

The protocol of the animal study performed in this research was approved by the Animal Care and Use Committee of Kaohsiung Medical University (IACUC-110029). Adult male Sprague–Dawley rats weighing approximately 250 g were provided by BioLASCO Taiwan (Taipei, Taiwan) and raised under a constant temperature and controlled illumination.

PASMC isolation and MCT-induced PAH-PASMCs

For PASMC isolation, the rats were sacrificed by anesthesia with an overdose of isoflurane, and all efforts were made to reduce their suffering. The skin of the rats was sterilized with 75% ethanol, and the chests were opened under sterile conditions. Then, the hearts and lungs were removed, and the pulmonary arteries were dissected. The PASMCs were then isolated as described previously [13]. PASMCs were cultured with Dulbecco's modified Eagle's medium (DMEM, 11966-025, Gibco, MA, U.S.A.) supplemented with 10% fetal bovine serum (FBS) and 1% antibiotic-antimycotic, 100× (15140122, Thermo Fisher Scientific, MA, U.S.A.) under 5% CO₂ at 37 °C. The PASMCs were examined by immunofluorescence staining to confirm their purity. Over 95% of the cells were composed of PASMCs. To obtain PAH-PASMCs from the animal disease model, a single injection of MCT (60 mg kg⁻¹) was administered to the rats via intraperitoneal injection for 4 weeks to develop PAH as described

previously [13], and the rats were then sacrificed for PASCs isolation for further experiments.

YULINK knockdown

Both the pGIPZ lentiviral shRNA vector packaged with a short hairpin RNA targeting *YULINK* (Clone ID. V3LHS_374795 and gene access no. NM_019005, respectively) and a nontargeting scramble control shRNA vector RHS4346 were purchased from Open Biosystems (AL, U.S.A.). PASCs were infected with the viruses with 8 µg/ml polybrene (MilliporeSigma, MA, U.S.A.) for 72 h and selected by using puromycin (2 µg/ml) to generate gene knockdown. Cells with *YULINK* knockdown were then maintained with media containing antibiotics.

YULINK overexpression

To generate *YULINK* overexpression, the full-length coding region of *YULINK* was constructed into a lentiviral pCDH-CMV-MCS-EF1α-copGFP vector (System Biosciences, CA, U.S.A.) and applied to PASCs with 8 µg/ml polybrene for 72 h. Puromycin (2 µg/ml) was used to select the cells that were successfully infected. Selected PASCs with *YULINK* overexpression were maintained in media containing antibiotics.

Transwell migration assay

A Transwell migration assay [14] was used to investigate PDGF-triggered and PAH-related cell migration. Briefly, PASCs were seeded into the upper compartment of Transwell chambers (3413, Corning Inc., NY, U.S.A.) with DMEM containing 2% FBS. The medium in the lower compartment contained 10% FBS with or without various doses of PDGF (5 ng/ml, 20 ng/ml). After 24 h, the cells were washed with PBS and fixed with 4% paraformaldehyde. The fixed cells were stained with crystal violet. The non-migrated cells were wiped off by using cotton swabs. The migrated PASCs were then recorded and photographed through a microscope.

PASC proliferation and viability analysis

MTT (3-(4,5-dimethylthiazol-2-yl)-2,5-diphenyltetrazolium bromide) was used to examine cell proliferation. After the treatments, PASCs were washed with PBS, and the culture medium was replaced with fresh medium containing 10 µg/ml MTT for 1 h. The purple-colored formazan crystals produced by living cells were dissolved in dimethyl sulfoxide (DMSO). Cell viability was then quantified by measuring the absorbance at a wavelength of 570 nm.

Western blot

As described previously [15], cell lysates were prepared and fractionated using sodium dodecyl

sulfate–polyacrylamide gel electrophoresis (SDS-PAGE) and blotted with antibodies. The Western Lightning® Plus-ECL detection system (NEL104001EA, PerkinElmer, MA, U.S.A.) was used to determine protein expression. The primary antibodies used were as follows: Mios (ab202274, Abcam, Cambridgeshire, U.K.), p-FAK Y397 (ab81298, Abcam), FAK (ab40794, Abcam), GLUT1 (73015, Cell Signaling, MA, U.S.A.), hexokinase II (2867, Cell Signaling), PDGFR (ab203491, Abcam), p-PI3k p85 Y458 + p55 Y199 (ab278545, Abcam), PI3k p85 (4292S, Cell Signaling), p-AKT S473 (4060, Cell Signaling), p-AKT T308 (13038, Cell Signaling), AKT (9272, Cell Signaling), and β-actin (3700, Cell Signaling). The secondary antibodies used were anti-rabbit IgG (7074, Cell Signaling) and anti-mouse IgG (7076, Cell Signaling). The Western blot results were further determined using ImageJ software and normalized with an internal control.

Flow cytometry analysis

After the treatments, both floating dead and attached living cells were collected and fixed with 70% ethanol to increase the permeability for later propidium iodide (PI) staining. Fixed cells were washed three times with PBS to remove ethanol before staining with PI. Meanwhile, RNaseA was used to eliminate any possibility of RNA interference. The cell cycle profile was analyzed by using an LSR II Flow Cytometer (BD Biosciences) and FlowJo 7.6 software (FlowJo LLC, OR, U.S.A.).

Glucose uptake analysis

In this study, glucose uptake was analyzed by using a Fluorometric 2-Deoxyglucose Assay Kit (KA3751, Abnova, Taipei, Taiwan). PASCs (2.5×10^4 cells/well) were seeded into a 24-well plate overnight to allow attachment. On the day of examination, 10% FBS regular culture medium was replaced with 0.5% FBS culture medium for a 1-hour starvation. Starved cells were then washed three times with PBS and treated with 10 mM 2-DG glucose uptake mix for 20 min. Afterwards, the cells were washed three times with PBS to remove exogenous 2-DG and lysed with 90 µl of extraction buffer. Cell lysates were cooled on ice for 5 min and neutralized with 10 µl of neutralization buffer followed by mixing with assay buffer at 37 °C for 40 min. The level of glucose uptake was determined by measuring fluorescence at Ex/Em = 535/587 nm.

Immunofluorescence assay

Cells were seeded on glass coverslips for the treatment. Afterwards, the cells were washed with PBS and fixed with 3% buffered paraformaldehyde for immunostaining. Fluorescence images of stained cells were recorded using a Zeiss Axioplan 2 Upright Fluorescence Microscope

and analyzed with Velocity 3.6.1 software (Improvision, West Midlands, U.K.). The primary antibodies were MIOS (ab122822, Abcam) and GLUT1 (ab40084, Abcam); the secondary antibodies were goat anti-rabbit IgG (H+L), F(ab')₂ fragment, CFTM568 (SAB4600400, Merck, Darmstadt, Germany), goat anti-mouse IgG (H+L), highly cross-adsorbed (min X Rat), CFTM568 (SAB4600311, Merck), and goat anti-rabbit IgG (H+L), highly cross-adsorbed, CFTM488 (SAB4600045, Merck). DAPI (4',6-diamidino-2-phenylindole) was used to stain the nuclei.

Glycolytic function analysis

During the process of glycolysis, glucose is catalyzed by enzymes and finally converted into pyruvic acid. In this research, we determined pyruvate production by using the Pyruvate Assay Kit (ab65342, Abcam) following the manufacturer's guidelines to examine the correlation between the level of YULINK and glycolysis in PSMCs. Briefly, 8×10^4 PSMCs with varying YULINK levels were seeded into a 96-well plate and treated with or without PDGF for 48 h, followed by measurement of pyruvate concentrations. The content of pyruvate was determined by measuring the fluorescence at Ex/Em=540/590 nm, which was generated by pyruvate oxidase via enzyme reactions.

Histological analysis

The procedures of the sample preparation were described previously [16]. Briefly, the bronchial artery tissue was fixed with 4% paraformaldehyde and embedded in paraffin wax before sectioning to 4 μ m-thick specimens for immunohistochemistry (IHC). Samples were deparaffinized and rehydrated with 100%, 95%, and 70% alcohol before being washed with distilled water. The samples were then stained with aniline blue solution and differentiated with 1% acetic acid solution. After incubation, the samples were washed with distilled water followed by dehydration with 95% and absolute ethyl alcohol. Finally, the samples were mounted with resinous mounting medium for later microscopy. Furthermore, we acquired a human right pulmonary artery specimen of an individual diagnosed with severe PAH, from Kaohsiung Medical University Hospital Biobank (approved by the Institutional Review Board of Kaohsiung Medical University Hospital, KMHIRB-E(I)-20230233) to assess YULINK expression in a clinical context. A normal pulmonary artery tissue was used as a control for comparative analysis.

For immunohistochemical analysis of increased levels of YULINK, YULINK (rabbit anti-MIOS, ab122822, Abcam) (1:100) antibody was selected for immunostaining. The images were recorded and analyzed using Motic

EasyScan One (Motic, Xiamen, China) and Motic DSAAssistant software.

Membrane protein extractions

A Mem-PERTM Plus Membrane Protein Extraction Kit (89842, Thermo Fisher Scientific) was used for membrane protein extraction. Cells were resuspended and collected for centrifugation at 300 \times g for 5 min. Cell pellets were further washed with Cell Wash Solution followed by another 5-min centrifugation at 300 \times g. Permeabilization buffer was added to the pellets for a 10-min incubation at 4 °C with constant mixing. Permeabilized cells were then centrifuged at 16,000 \times g for 10 min to remove cytosolic fractions. Solubilization buffer was added to the samples for a 30-min incubation at 4 °C with constant mixing. Membrane proteins were finally isolated and extracted after a 15-min centrifugation at 16,000 \times g at 4 °C.

Immunoprecipitation analysis

The immunoprecipitation analysis was conducted using the Pierce Crosslink Magnetic IP/Co-IP Kit (Thermo Fisher Scientific, 88805) in accordance with the manufacturer's instructions. Prior to antigen immunoprecipitation, the YULINK antibodies were crosslinked to magnetic beads using DSS. Cell protein lysates, prepared in advance, were then incubated with the antibody-crosslinked beads at room temperature to facilitate the elution of bound antigens.

Statistical analysis

SPSS 17.0 (one-way ANOVA followed by post hoc analysis with the Bonferroni correction; SPSS Inc., IL, U.S.A.) was used for statistical analysis. All represented results in this study are derived from at least three independent repeats. Values are presented as the mean \pm S.D. A *p* value < 0.05 indicates a statistical significance between compared groups.

Results

Positive correlation between YULINK expression and cell migration in PSMCs

To evaluate the role of YULINK in PSMC migration in either *YULINK* knockdown (KD) or overexpression (OE), PSMCs were analyzed by Western blot analysis, with the efficiency shown in Fig. 1A, B, respectively. To further examine whether diminished YULINK expression could inhibit PSMC migration, PSMCs with or without *YULINK* knockdown were seeded on the permeable upper layer of the cell culture with a dose-dependent PDGF (0, 5, 20 ng/ml) treatment in the culture medium on the bottom layer of the well for cell migration analysis. As shown in Fig. 1C, PSMC

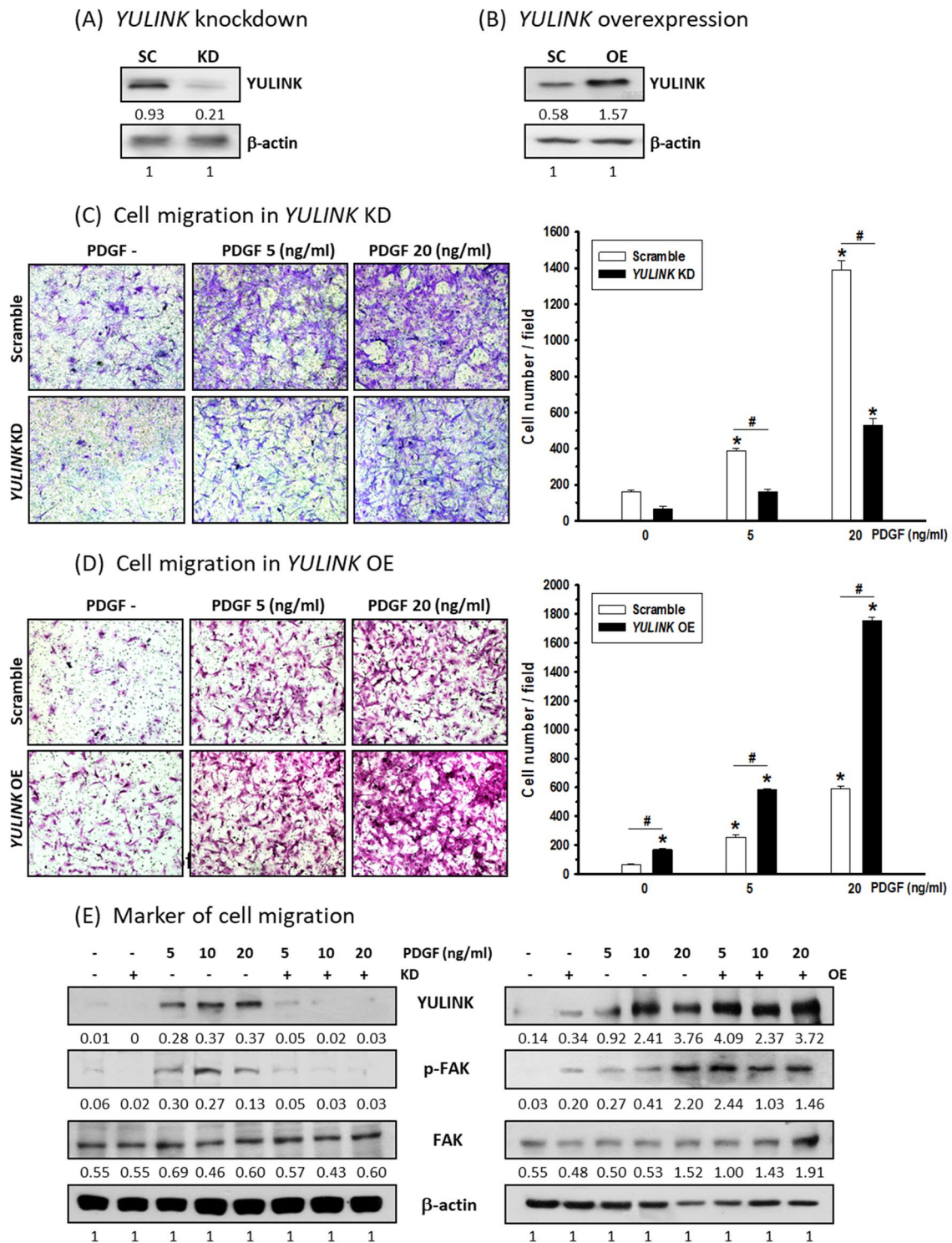


Fig. 1 Positive correlation between YULINK expression and cell migration in PSMCs. YULINK expression in PSMCs with **A** YULINK knockdown (KD) or **B** overexpression (OE) was examined by western blot analysis. SC stands for scramble control. The numbers labeled below the respective blot lanes indicate the relative fold normalized with the internal control. **C, D** Micrographs (magnification 200x) together with bar graphs depict PDGF (5 and 20 ng/ml)-triggered cell migration in PSMCs with **C** YULINK KD or **D** YULINK OE using Transwell analysis. The values represent the mean of three independent experiments \pm standard deviation. * $p < 0.05$ compared to scramble control without PDGF. # $p < 0.05$ between compared groups. **E** PSMCs with or without YULINK KD or OE were treated with PDGF in a dose-dependent manner (0, 5, and 20 ng/ml) for 24 h and subjected to western blot analysis for the indicated proteins. β -actin served as an internal control

migration increased in a dose-dependent manner. Cell migration was significantly reduced in YULINK-deficient PSMCs treated with PDGF, while in contrast, cell migration was enhanced in PSMCs overexpressing YULINK with or without PDGF treatment (Fig. 1D).

Furthermore, focal adhesion kinase (FAK), a protein that is well recognized as a marker of cell migration, was also determined by Western blot analysis. In addition, FAK is widely expressed as a cytoplasmic protein tyrosine kinase and plays an important key step in cell migration when activated by phosphorylation at Tyr397 [17]. As shown in Fig. 1E, the administration of PDGF induced either YULINK or FAK phosphorylation at Tyr397 in a dose-dependent manner; however, this PDGF-triggered enhancement of FAK phosphorylation was inhibited in PSMCs with YULINK knockdown. In contrast, FAK Tyr397 phosphorylation in response to PDGF treatment was enhanced in PSMCs overexpressing YULINK (Fig. 1E). These data illustrate that YULINK could be a positive regulator in PSMCs under PDGF treatment.

Positive correlation between YULINK expression and cell proliferation in PSMCs

To investigate whether the YULINK expression level could affect cell proliferation, PSMCs with YULINK knockdown (KD) or overexpression (OE) in response to PDGF (20 ng/ml) at 0 and 5 days were subjected to MTT proliferation/viability analysis (Fig. 2A), with increased cell proliferation being noted in PSMCs with PDGF for 5 days compared to those without PDGF treatment. Cell proliferation was inhibited in PSMCs with YULINK KD with or without PDGF treatment. In contrast, cell proliferation was enhanced in PSMCs with YULINK OE with or without PDGF treatment. Similarly, the colony formation assay provided additional evidence of the relationship between YULINK expression and cell proliferation. In the presence of PDGF treatment or in PAH-PSMCs, numerous and distinct colonies formed. However, when YULINK was preemptively suppressed, the colony formations were noticeably reduced (Additional file 1: Fig. S1).

As shown in Fig. 2B, these results were further confirmed by cell cycle profile analysis. Both floating and attached cells were collected and stained with propidium iodide (PI) for DNA content detection. In comparison to the scramble control, treatment with PDGF triggered a significant increase in the S-phase population, indicating further DNA synthesis for cell proliferation; however, this upregulated S-phase population was not found in PSMCs with YULINK knockdown. Even without PDGF treatment, PSMCs with YULINK knockdown

or overexpression alone slightly suppressed or increased the S-phase population, respectively, accompanied by an increased or decreased G1 phase population, respectively.

Furthermore, existing researches have indicated that PAH pathogenesis involves genomic instability, the production of free radicals, and elevated levels of DNA damage [13, 18], which can lead to apoptosis. However, this effect is likely transient, as cells eventually tend to exhibit increased proliferation during PAH pathogenesis. It is evident that in PSMCs treated with PDGF, there was an increase in the subG1 population, which was further elevated in cells with YULINK overexpression. However, when YULINK was inhibited, this elevation in the subG1 population was significantly mitigated. These results align with the notion that YULINK overexpression, particularly in conjunction with PDGF treatment, leads to genome instability and cell death associated with PAH. This finding also suggests that the inhibition of YULINK could be advantageous in suppressing the pathogenesis of PAH. Taken together, the cell proliferation of PSMCs was positively correlated with YULINK under PDGF treatment.

YULINK colocalized with GLUT1 and participated in PDGF-triggered glucose uptake and glycolysis

Increased glucose uptake and glycolysis in both pre-clinical studies and PAH patients were noted in hyper-proliferative PSMCs, which have increased GLUT1 1 expression [19–21]. Therefore, one of our goals was to investigate whether YULINK expression was related to either glucose uptake or glycolysis in PSMCs. PSMCs were treated with the fluorescent glucose analog 2-deoxy-D-glucose (2-DG) to determine the levels of glucose uptake in response to PDGF treatment. Since the 2-hydroxyl group of 2-DG is replaced by hydrogen, it would be transported and thereby accumulate in cells without entering glycolysis, so the fluorescence of accumulated 2-DG would indicate the level of glucose uptake. As shown in Fig. 3A, glucose uptake was inhibited in PSMCs with YULINK knockdown compared to the scramble control. In contrast, glucose uptake was enhanced in PSMCs with YULINK overexpression, while PDGF administration promoted glucose uptake in PSMCs, which was inhibited in PSMCs with YULINK knockdown. On the other hand, glucose uptake was further enhanced in PSMCs overexpressing YULINK under PDGF treatment (Fig. 3A).

We next examined whether YULINK expression was correlated with glycolysis in PSMCs. PSMCs with YULINK knockdown or overexpression were collected for pyruvate production under PDGF treatment for 48 h, and as shown in Fig. 3B, pyruvate production was significantly increased in PSMCs under PDGF treatment,

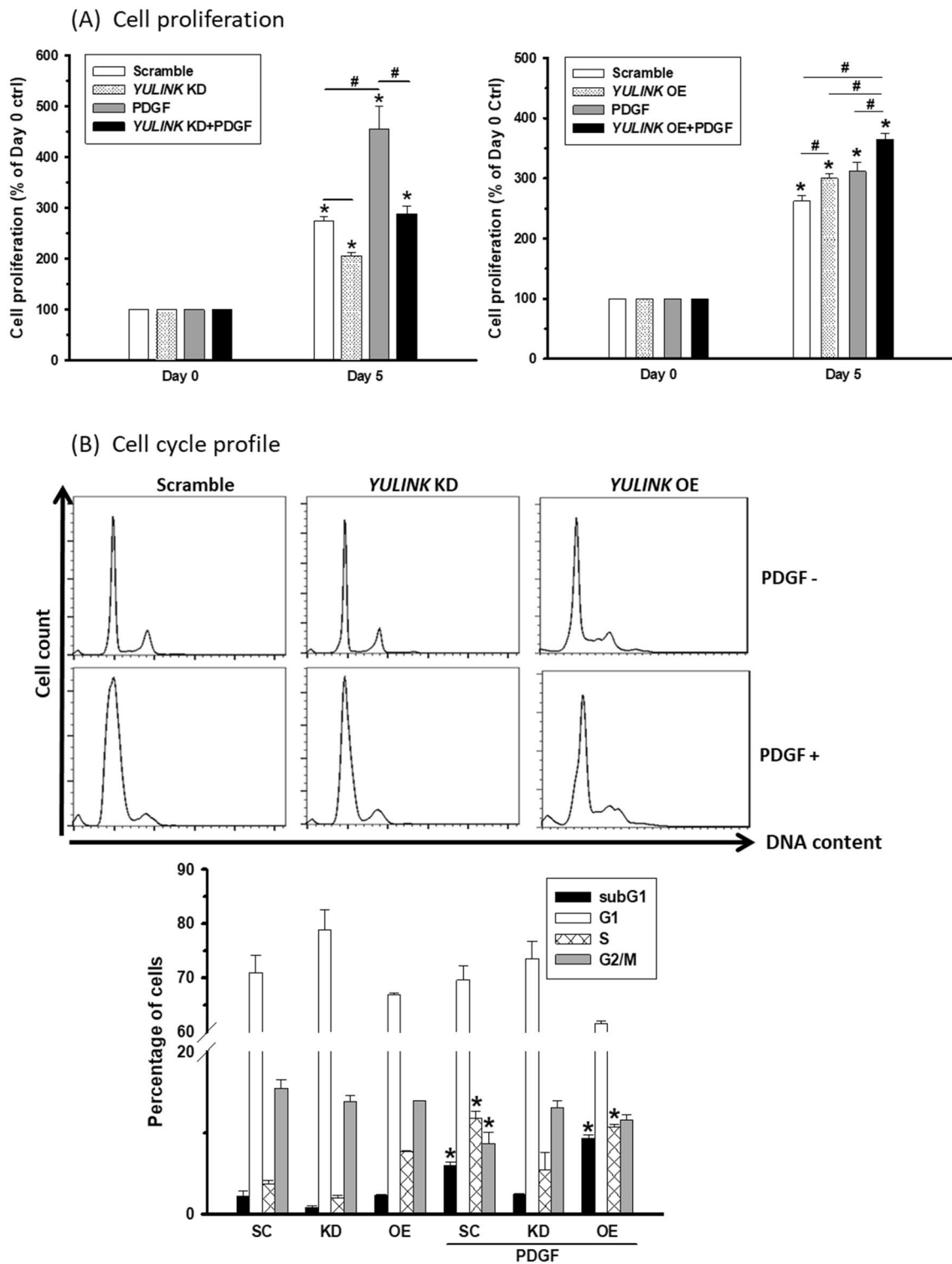


Fig. 2 Positive correlation between YULINK expression and cell proliferation in PSMCs. **A** PSMCs with YULINK KD or OE were treated with or without PDGF (20 ng/ml) for 5 days before harvest for MTT analysis. **B** PSMCs with the same treatment for 24 h were stained with PI and subjected to flow cytometry. The cell cycle profiles are presented with bar graphs indicating the distributions of the cells in the cell cycle. The values represent the mean of three independent experiments \pm standard deviation. * $p < 0.05$ compared to scramble control without PDGF. # $p < 0.05$ between compared groups

which indicated an upregulation of glycolysis. Furthermore, pyruvate production was further enhanced in PSMCs with *YULINK* overexpression under PDGF treatment, but in contrast, pyruvate production was inhibited in either PDGF-treated or no-PDGF-treated PSMCs with *YULINK* knockdown.

Since glucose transporter 1 (GLUT1), the major member of the Glut family, was reported to be expressed in vascular smooth muscle cells and facilitate glucose uptake for vascular contractility and reactivity [22], we next examined whether the alteration of *YULINK* expression further affected GLUT1 expression. Consistently, while *YULINK* knockdown decreased GLUT1 expression in PSMCs, the level of GLUT1 was increased with *YULINK* overexpression regardless of the presence or absence of PDGF treatment (Fig. 3C). Additionally, the level of hexokinase II (HK-2), the key catalytic kinase that converts glucose to glucose-6-phosphate in the process of glycolysis, was affected in the same pattern as GLUT1 by western blotting analysis (Fig. 3C).

To investigate whether *YULINK* and GLUT1 had protein interactions under PDGF treatment, immunofluorescent analysis was performed for PSMCs with or without PDGF treatment. As shown in Fig. 3D, GLUT1 and *YULINK* were not only increased but also colocalized in PSMCs treated with PDGF. Taken together, *YULINK* expression could regulate glucose uptake and glycolysis through GLUT1 protein interaction under PDGF treatment, thereby implying a possible role of *YULINK* in PAH-related pathogenesis.

In addition to PDGF-treated PSMCs, PSMCs derived from monocrotaline-induced PAH rat models were also examined. As shown in Additional file 1: Fig. S2, medial hypertrophy was noted by hematoxylin and eosin (H & E) staining of the pulmonary artery in the MCT-induced PAH group, confirming the efficacy of the MCT treatment. Since GLUT1 is known to localize on the cell membrane and functions as a glucose transporter, we conducted further investigations to determine whether *YULINK* also exhibits an increase in cell

membrane localization in PSMCs during PAH pathogenesis. As shown in Fig. 3E, F, increased *YULINK* expression was noted in both whole-cell lysates and membrane fractions in PSMCs under PDGF treatment and in PAH-PSMCs. A co-immunoprecipitation analysis provided further evidence of the colocalization of *YULINK* and GLUT1 on the cell membrane in PSMCs. Under the conditions related to PAH pathogenesis, it was evident that GLUT1 was notably present in the protein extracts that were pulled down along with *YULINK* (Fig. 3G). These findings suggested that *YULINK* could be increased in the cell membrane of PSMCs for protein interaction with GLUT1 during PAH pathological development.

Enhanced *YULINK* expression in MCT-induced PAH rats and a clinical PAH patient

How *YULINK* is expressed in MCT-induced rats in vivo was next examined. Immunohistochemical (IHC) staining of the pulmonary artery in the MCT-induced PAH group revealed increased brown staining in the thickening vasculature of the pulmonary artery compared to the normal control. In normal animals, *YULINK* expression is minimal within the pulmonary artery. However, following PAH induction, there is a significant increase in the expression of *YULINK*, and it is distributed more extensively throughout the tissue including in media muscular layer (Fig. 4A), which indicated increased *YULINK* expression in the pulmonary artery of the MCT-induced PAH rat model.

In addition to the animal model, we obtained a human right pulmonary artery specimen of an individual with severe PAH and performed immunohistochemistry (IHC) staining to analyze *YULINK* expression in an actual clinical case. Consistent with the results observed in rat tissue, our findings in the human specimen also demonstrate a significant increase in *YULINK* expression particularly in media muscular layer in the human PAH specimen compared to the control from a normal pulmonary artery specimen (Fig. 4B).

(See figure on next page.)

Fig. 3 *YULINK* interacted with GLUT1 and participated in PDGF-triggered glucose uptake and glycolysis. The bar graphs illustrate **A** glucose uptake and **B** pyruvate production in PSMCs with *YULINK* KD or OE treated with or without PDGF (20 ng/ml) for 24 h. The values represent the mean of three independent experiments \pm standard deviation. * $p < 0.05$ compared to scramble control without PDGF. # $p < 0.05$ between compared groups. **C** Western blot analysis indicates the expression of GLUT1 and HK-2 in normal PSMCs, PSMCs with *YULINK* KD, and PSMCs with *YULINK* OE treated with or without PDGF for 24 h. The numbers labeled below the respective blot lanes indicate the relative fold normalized with the internal control. **D** Representative images from immunofluorescence analysis indicate the expression of *YULINK* (green) and GLUT1 (red), and DAPI (blue) indicates nuclear staining. Magnification 200 \times . **E** Whole-cell lysates and **F** membrane fractions derived from PSMCs or PAH-PSMCs with or without 20 ng/ml PDGF treatment and PAH-PSMCs were subjected to Western blot analysis for *YULINK* expression. β -Actin and Na/K ATPase served as internal controls. **G** Membrane protein lysates obtained from PSMCs subjected to indicated treatments were used for immunoprecipitation with *YULINK* antibody-conjugated beads. The proteins pulled down were subsequently analyzed via Western blot to assess the expression of *YULINK* and GLUT1. While Input serves as positive control, Isotype IgG serves as negative control

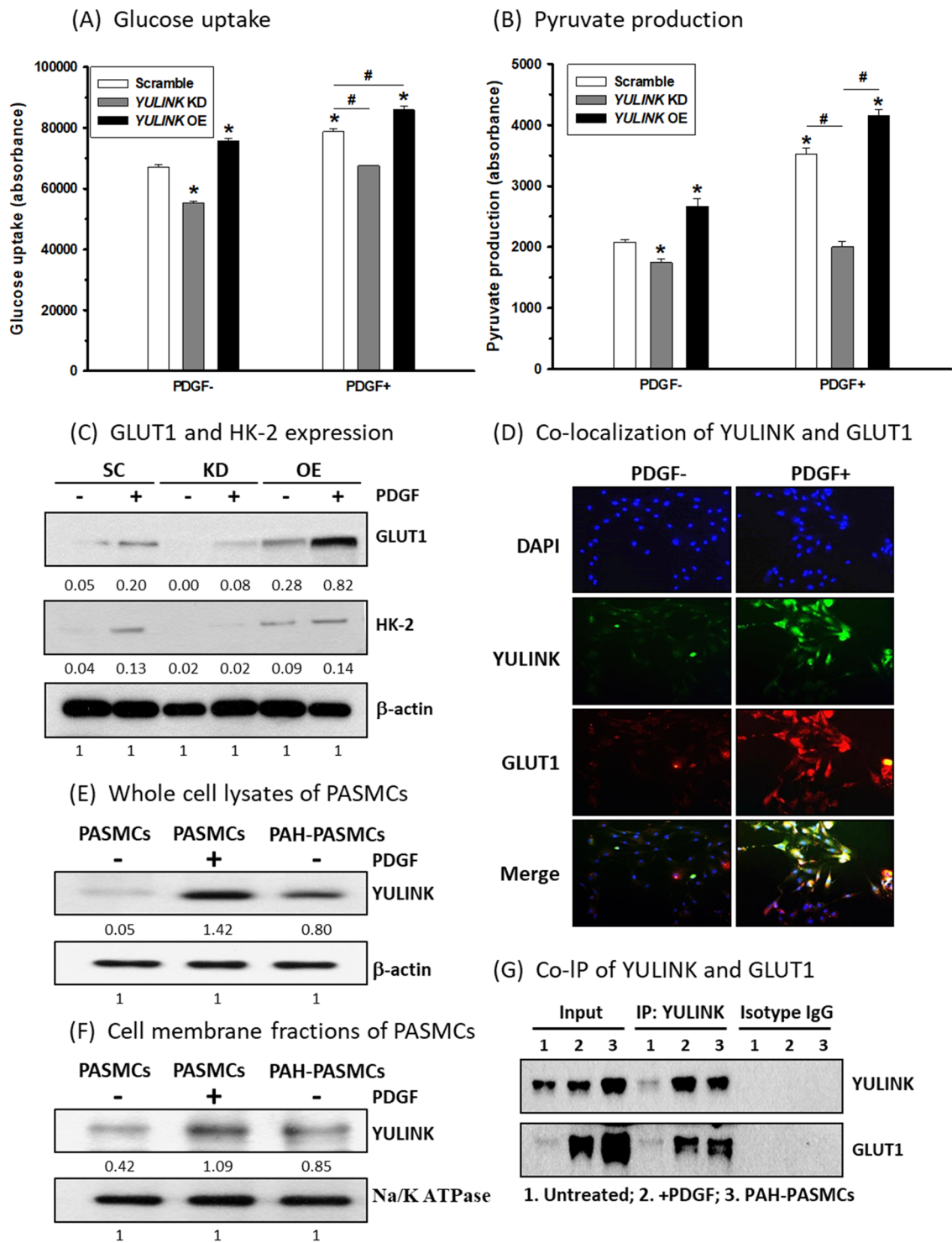
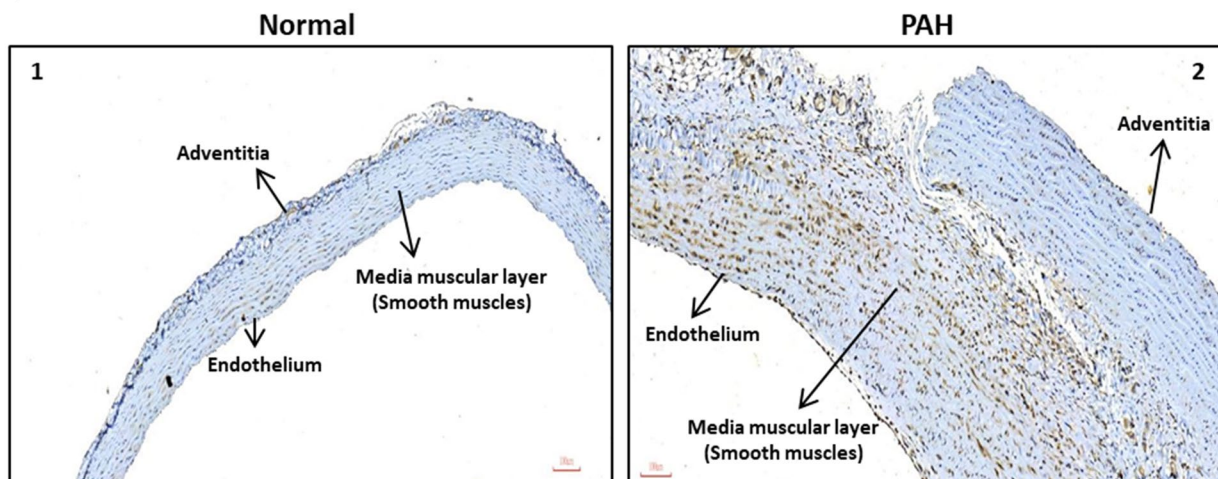


Fig. 3 (See legend on previous page.)

(A) Rat, YULINK



(B) Human, YULINK

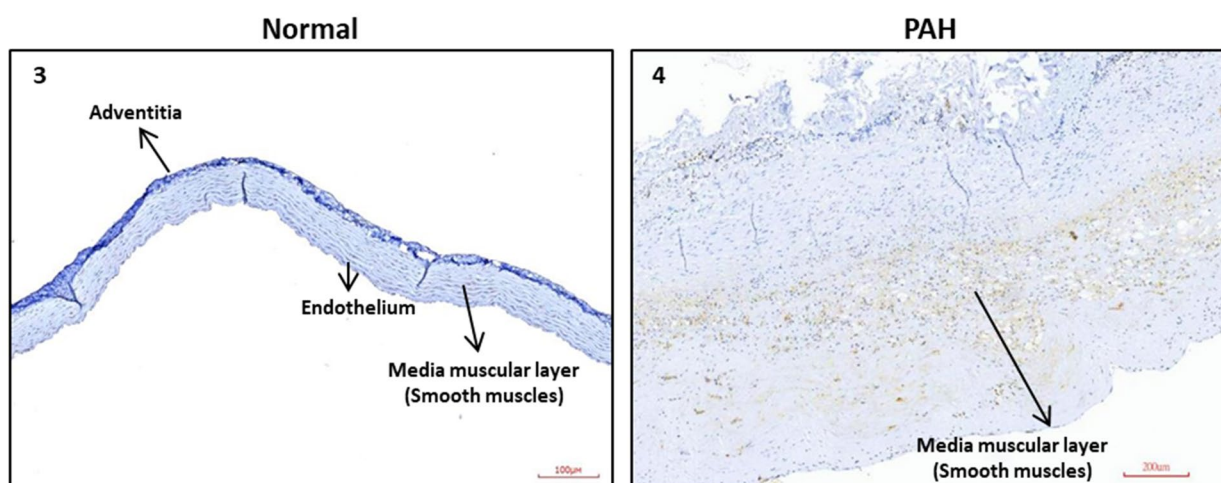


Fig. 4 Enhanced YULINK expression in MCT-induced PAH rats and human PAH specimen. **A** Pulmonary artery tissues were derived from normal and MCT-induced PAH rats for IHC staining. The brown color in the photomicrograph indicates the expression of YULINK expression. **B** Tissue sample from the right pulmonary artery of a clinical patient with severe PAH was subjected to IHC staining to assess YULINK expression. A normal pulmonary artery tissue was used as a control for comparison. Scale bar in 1–3: 100 μ m, and 4: 200 μ m

YULINK suppression inhibited the migration and proliferation of PSMCs derived from an MCT-induced PAH rat model (PAH-PSMCs)

To investigate whether cell migration and proliferation could be correlated with YULINK expression in PAH-PSMCs, cells with or without YULINK knockdown were analyzed by Transwell migration and proliferation assays. In comparison with PSMCs derived from normal rats, PAH-PSMCs exhibited a four- to five-fold increase in cell migration (Fig. 5A). However, when YULINK was knocked down, the cell migration was dramatically reduced by half in PAH-PSMCs (Fig. 5A);

furthermore, as shown in Fig. 5B, increased expression of YULINK and FAK phosphorylation were noted in PAH-PSMCs compared with PSMCs and were further enhanced by PDGF treatment in both PSMCs and PAH-PSMCs, although both were inhibited in PAH-PSMCs with YULINK knockdown.

Consistently, cell proliferation was enhanced by 50% in a 5-day proliferation analysis in PAH-PSMCs compared to PSMCs; however, cell proliferation was inhibited in PAH-PSMCs with YULINK knockdown (Fig. 5C). As shown in Fig. 5D, pyruvate production increased in PAH-PSMCs, which indicated increased

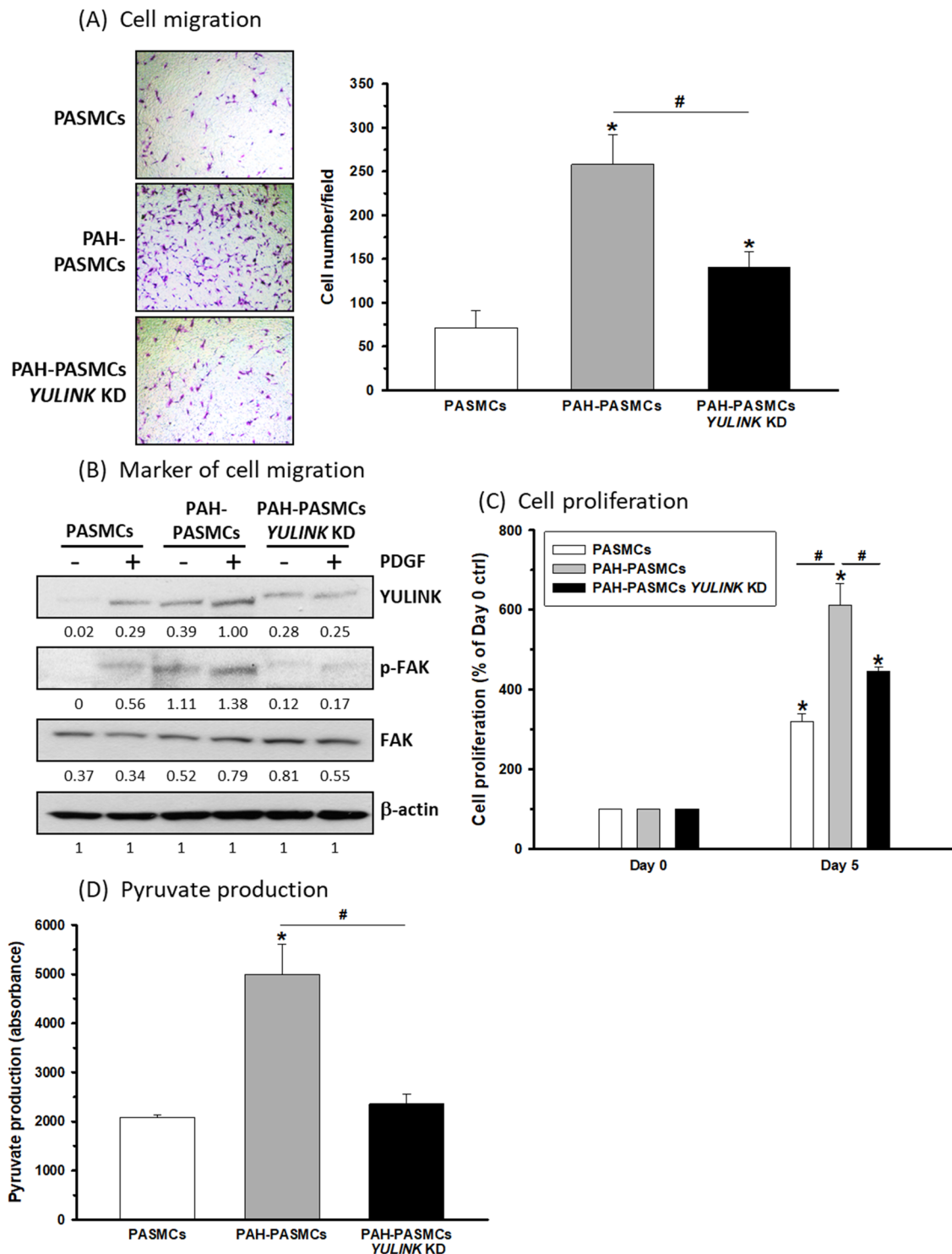


Fig. 5 YULINK knockdown reversed the enhancement of cell migration and proliferation in PAH-PASMCs. PASMCs and cells derived from MCT-induced PAH rats with or without YULINK KD were prepared for Transwell cell migration analysis. **A** Microscopy images presented with bar graphs indicate cell migration in PASMCs. Magnification $\times 200$. **B** The cells were incubated with PDGF (20 ng/ml) for 24 h before harvest for protein extractions. Western blot analysis indicates the activation and expression of the indicated proteins. β -actin served as an internal control. The numbers labeled below the respective blot lanes indicate the relative fold normalized with the internal control. **C** MTT analysis of the 5-day proliferation of the cells. **D** The production of pyruvate in the cells. The values represent the mean of three independent experiments \pm standard deviation. * $p < 0.05$ compared to normal PASMCs. # $p < 0.05$ between compared groups

glycolysis compared to that in PSMCs, whereas it decreased in PAH-PSMCs with *YULINK* knockdown compared to that in PSMCs. Taken together, PAH-PSMCs revealed increased cell migration, proliferation and glycolysis compared to PSMCs, which could be associated with *YULINK* expression.

***YULINK* participated in cell migration and proliferation of PSMCs via the PI3K-AKT signaling pathway**

The phosphoinositide 3-kinase (PI3K)-protein kinase B (AKT) signaling pathway is one of the major downstream effects of the PDGF signaling pathway [23] and has been demonstrated to play an essential role in PDGF-induced PSMC proliferation, migration, and PAH progression [8, 24]. To explore the role of *YULINK* and its potential mechanism in PAH-related cell migration and proliferation, PSMCs derived from normal or MCT-induced PAH rats with or without *YULINK* knockdown were treated with PDGF for further experiments. As shown in Fig. 6A, the expression of *YULINK* and PDGFR was enhanced in PSMCs and PAH-PSMCs under PDGF treatment. Increased PI3K and AKT phosphorylation in response to PDGF treatment was found in the western blotting analysis, which indicated that PI3K-AKT signaling was activated in PSMCs and PAH-PSMCs under PDGF treatment. When *YULINK* was suppressed in PAH-PSMCs, the expression of PDGFR and the phosphorylation of PI3K and AKT were both inhibited with or without PDGF treatment.

To further examine whether *YULINK* could be involved in PSMC migration and proliferation via PI3K-AKT signaling, a PI3K inhibitor, LY294002, was administered to PSMCs with or without *YULINK* overexpression and PAH-PSMCs for further analysis. As shown in Fig. 6B, while treatment with LY294002 alone significantly reduced cell migration in PSMCs, the cell migration ability was rescued in PSMCs with *YULINK* overexpression under LY294002 treatment. In Fig. 6C, similar results were found in the cell proliferation experiment, with a 5-day proliferation assay showing significant inhibition of PSMC proliferation under LY294002 treatment. Furthermore, the downregulated cell proliferation induced by LY294002 treatment was restored in PSMCs overexpressing *YULINK*.

Taken together, the cell migration and proliferation of PSMCs under PDGF treatment or PAH-PSMCs might be regulated by *YULINK* through the PI3K-AKT signaling pathway.

Discussion

Despite advances in modern medicine, PAH is still a life-threatening and challenging disease, so lung transplantation could be the only solution for patients with

end-stage PAH. Three cellular signaling pathways, endothelin, nitric oxide/cyclic guanosine monophosphate (cGMP) signaling and prostacyclin pathways, have been utilized in the current treatment of PAH in such patients [25]. Nonetheless, existing therapeutic strategies like sildenafil [26], one of the most common treatments for PAH in clinical practice, predominantly target symptomatic relief through nitric oxide-induced vasodilation. Although these approaches can temporarily alleviate disease progression and improve quality of life [26], they are not curative and do not significantly impact mortality, particularly in severe cases.

Pulmonary vascular remodeling caused by aberrant cell migration and proliferation of PSMCs is the major pathological feature of PAH [27], so pharmacological approaches targeting cell migration and proliferation have been widely applied as a therapeutic strategy for PAH [28]. For example, the authors recently found that B-type natriuretic peptide inhibits angiotensin II-induced PSMC proliferation and migration via the cGMP/PKG pathway, which might show therapeutic potential for PAH therapy [29]. However, the genetic role for mediating pulmonary vascular remodeling has not been fully elucidated. In this study, we demonstrated that *YULINK* overexpression enhanced PDGF-induced PSMC migration through FAK activation; similarly, *YULINK* promoted proliferation and DNA synthesis in the cell cycle of PSMCs. As a result, *YULINK* might play various roles in the remodeling mechanisms of PAH.

Accelerated glycolysis, a cancer-like glucose metabolic reprogramming, has recently been noted as a unique feature in PAH pathogenesis. Positron emission tomography scans have shown that PDGF uptake is increased in both animal models and patients with PAH [14], so targeting a regulator that participates in glycolysis has been considered a potential promising approach in PAH therapeutics. The present study demonstrated that *YULINK* was involved in glycolysis, including glucose uptake, GLUT1 expression, HK-2 expression and pyruvate production, through GLUT1 interaction; additionally, the expression of HK-2 in PSMCs was decreased when *YULINK* was suppressed. Among the four isoforms of hexokinase, studies have revealed that the activity of HK-2 is significantly increased in rapidly growing cells compared with normal cells and plays a first rate-limiting role in glycolysis for energy supply in abnormally proliferating cells [27, 28]. Our results are in line with a previous study targeting HK-2 by using the noncoding microRNA miR125a-5p to inhibit glycolysis as an approach to improve PAH [29]. Therefore, *YULINK* could be a promising target for glycolysis in the management of PAH.

This study demonstrated that enhanced *YULINK* expression was found in PDGF-treated PSMCs,

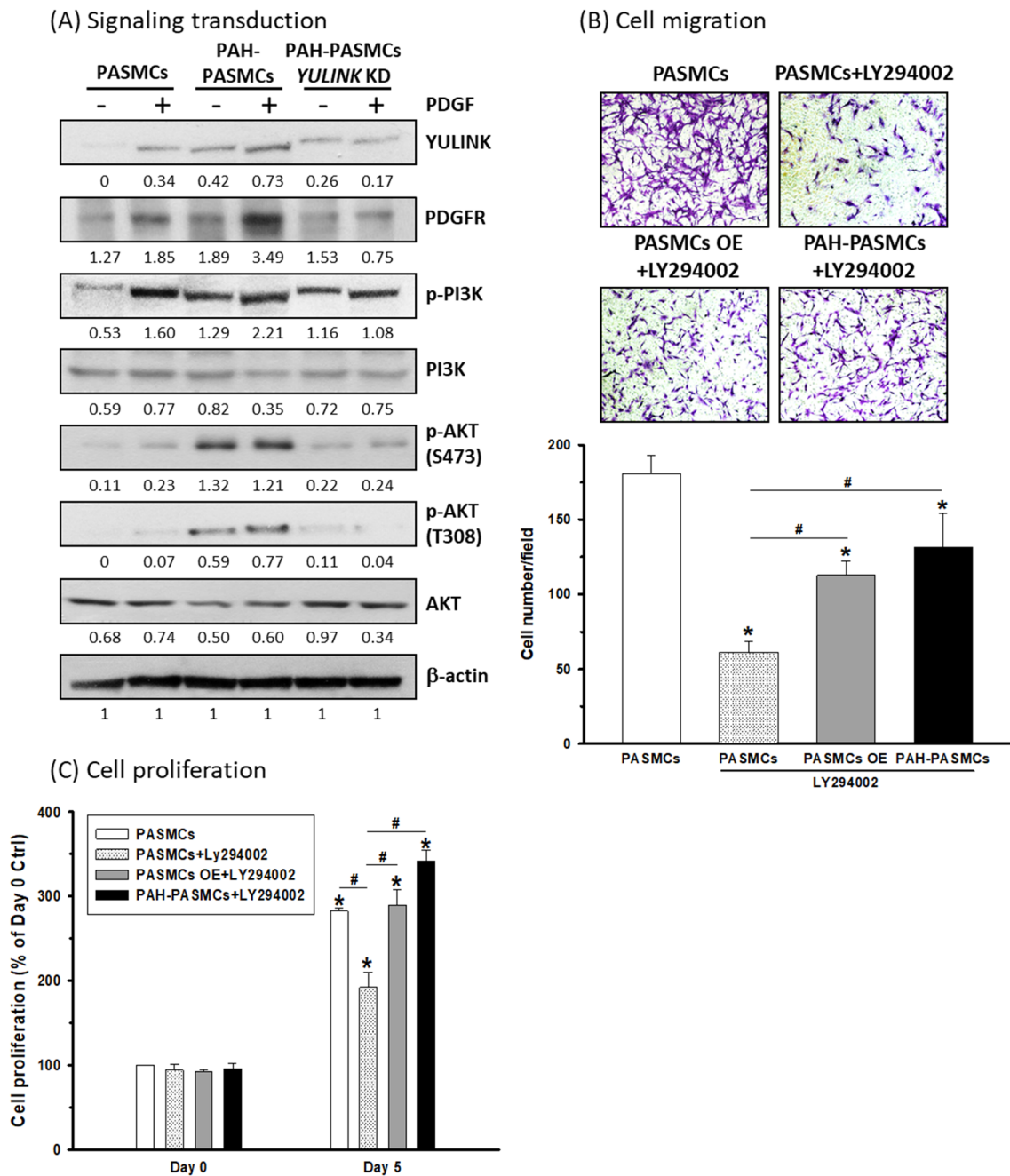


Fig. 6 YULINK regulated cell migration and proliferation in PASCs via PI3K-AKT signaling. **A** PASCs and PAH-PASCs with or without YULINK KD were treated with or without 20 ng/ml PDGF for 24 h for protein extraction. Cell lysates were subjected to western blot analysis for the indicated proteins. β-Actin served as an internal control. The numbers labeled below the respective blot lanes indicate the relative fold normalized with the internal control. **B** Representative images (magnification 200×) together with the bar graphs indicate the cell migration analysis of PASCs, PASCs with or without YULINK OE treated with LY294002 (10 μM), and PAH-PASCs treated with LY294002. **C** A 5-day cell proliferation assay in the cells under the indicated treatments. *p < 0.05 compared to control PASCs. #p < 0.05 between compared groups

PASCs and pulmonary arteries of MCT-induced PAH rats, and the pulmonary arteries of a patient specimen. PDGF and its receptor PDGFR have been reported to coordinately regulate pulmonary vascular remodeling

by mediating cell proliferation and migration, which are key mechanisms mediating PAH pathogenesis [30]. Therefore, targeting PDGFR by receptor tyrosine kinase inhibitors such as imatinib is considered a new intriguing

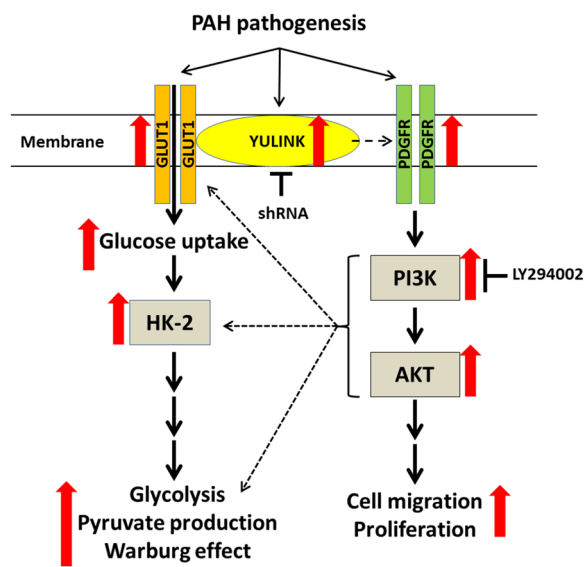


Fig. 7 Putative roles of YULINK in PDGF- or MCT-induced PAH pathological aberrations. During PAH-related pathogenesis induced by PDGF or MCT, an increase in YULINK expression occurs. YULINK coordinates with GLUT1 to facilitate glucose uptake, accompanied by an upregulation of HK-2, promoting enhanced glycolysis in PSMCs. This increased YULINK expression also contributes to uncontrolled cell migration and proliferation through the PDGFR-PI3K-AKT signaling pathways. While numerous reports have highlighted the role of this pathway in glucose metabolism and the Warburg effect, whether the triggered PI3K-AKT signaling regulates PAH-related processes requires further investigation. Suppression of YULINK through gene knockdown or the use of an inhibitor LY294002 to suppress PI3K activation has the potential to reverse these pathological abnormalities associated with PAH. In this graph, the black arrows represent the signaling transduction pathways, and the red arrows denote the enhancements in response to PAH pathogenesis. The dotted lines summarize findings from other published literature, not experiments conducted in this manuscript

strategy to treat PAH [31]. Administering imatinib not only reversed experimental pulmonary hypertension in an animal disease model but also improved outcomes in patients with end-stage PAH [32]. In our results, suppressing YULINK significantly reversed cell migration and proliferation of PSMCs not only in PDGF treatment but also in MCT-induced PAH rats. Our findings suggest that YULINK may serve as another attractive target in PAH-targeted therapy.

Furthermore, published reports support the importance of PI3K-AKT in pulmonary vascular remodeling and the pathological development of PAH. The PI3K-AKT pathway is another signaling cascade that has been well demonstrated to contribute to cell migration and proliferation in various cell types, including PSMCs, in PAH [30]. PI3K-AKT inhibition using a small molecular inhibitor, LY294002, can reverse hypoxia-induced anti-apoptosis and PSMC proliferation under hypoxic

conditions [31–33]. Pharmacological experiments using multi-kinase inhibitors such as sorafenib in animal models also showed therapeutic benefits in reversing the development of MCT-induced PAH [12]. Knockout of AKT1 in mice was also demonstrated to attenuate vascular remodeling and exhibited a protective effect against the development of hypoxia-induced pulmonary hypertension [34]. Furthermore, the PI3K-AKT pathway has been reported to be involved in glucose metabolism, particularly in regulating GLUT1 and hexokinase 2 to mediate glycolysis in various types of cancer [35–37]. This pathway has also been shown to promote the Warburg effect in PSMCs in response to PDGF stimulation [8]. Although further investigation is required, it may exhibit similar regulatory mechanisms in PAH pathogenesis due to the shared characteristics between cancer and PAH development.

Conclusions

Our results demonstrate that YULINK inhibition decreased the expression of PDGFR or the activation of PI3K-AKT signaling in PSMCs with PDGF treatment or PAH-PSMCs; furthermore, the inhibition of cell migration and proliferation by LY294002 treatment was significantly reversed in PSMCs with YULINK overexpression or PAH-PSMCs, so the PDGF/PI3K/AKT axis is involved in the effects of YULINK on the pathophysiological development of PAH. Since aberrant proliferation and migration of PSMC, and dysregulated glucose metabolism are the major reasons for PAH, our study indicates that YULINK plays a crucial role in the migration, proliferation and glycolysis of PSMCs, as shown in Fig. 7. Consequently, targeting YULINK holds promise as a potential therapeutic strategy for the treatment of PAH. Further animal and clinical studies are needed to substantiate these important findings.

Abbreviations

PASMCs	Pulmonary arterial smooth muscle cells
PAH	Pulmonary arterial hypertension
Mios	Meiosis Regulator for Oocyte Development
PDGF	Platelet-derived growth factor
DMEM	Dulbecco's modified Eagle's medium
FBS	Fetal bovine serum
PBS	P
	hosphate-buffered saline
ANOVA	Analysis of variance
PDGFR	Platelet-derived growth factor receptor
MCT	Monocrotaline
GLUT1	Glucose transporter 1
HK-2	Hexokinase II
mPAP	Mean pulmonary artery pressure
mTOR	Mammalian target of rapamycin
PI3K	Phosphoinositide 3-kinase
KD	Knockdown
PI	Propidium iodide
2-DG	2-Deoxyglucose

Ex/Em Excitation/emission
 eNAMPT Extracellular nicotinamide phosphoribosyltransferase
 HMGB-1 High mobility group box 1

Supplementary Information

The online version contains supplementary material available at <https://doi.org/10.1186/s40659-023-00480-z>.

Additional file 1: Figure S1. Colony formation analysis. A total of 3×10^2 PASCs, with their respective treatments as indicated, were seeded into six-well plates and allowed to grow for 10 days. The formed colonies were then fixed with 4% paraformaldehyde and stained with crystal violet.

Figure S2. Morphological changes of pulmonary artery in MCT-induced PAH rats. Tissues of pulmonary artery were derived from normal and MCT-induced PAH rats respectively, for Hematoxylin & Eosin staining. Representative photomicrographs indicate the MCT-induced morphological changes in the tissues of pulmonary artery. Magnification 200 \times .

Acknowledgements

We would like to express our gratitude to Professor John Yu (Institute of Stem Cell and Translational Cancer Research, Chang Gung Memorial Hospital, Taiwan) for consultation and to Mr. Yu-Sen Liu and the Center for Research Resources and Development (CCRD) of Kaohsiung Medical University for technical assistance. Furthermore, the authors thank the Center for Laboratory Animals in Kaohsiung Medical University for the animal care.

Author contributions

Conceptualization: YW; methodology: YW and WW; validation: WW; formal analysis: WW; investigation: WW; resources: MY, YS, JY; data curation: WW; writing—original draft preparation: WW; writing—review and editing: YW, WW, and JH; supervision: JW; project administration: JW; funding acquisition: YW and JW. All authors have read and agreed to the published version of the manuscript.

Funding

This research was supported by research grants from the National Science and Technology Council, Taiwan (MOST 110-2314-B-650-005, MOST 111-2314-B-650-003), Kaohsiung Medical University (KT112P001), and E-Da Hospital (EDPJ-111048).

Availability of data and materials

Not applicable.

Declarations

Ethics approval and consent to participate

Not applicable.

Consent for publication

Not applicable.

Competing interests

The authors declare no conflicts of interest.

Author details

¹Division of Plastic Surgery, Department of Surgery, Kaohsiung Medical University Hospital, Kaohsiung Medical University, Kaohsiung 80708, Taiwan. ²Department of Plastic Surgery, Kaohsiung Municipal Ta-Tung Hospital, Kaohsiung 80145, Taiwan. ³Department of Surgery, School of Medicine, Kaohsiung Medical University, Kaohsiung 80708, Taiwan. ⁴Regenerative Medicine and Cell Therapy Research Center, Kaohsiung Medical University, Kaohsiung 80708, Taiwan. ⁵Department of Pediatrics, E-Da Hospital/I-Shou University, No. 1, Yi-Da Road, Jiao-Su Village, Yan-Chao District, Kaohsiung 82445, Taiwan. ⁶Department of Pediatrics, School of Medicine, College of Medicine, I-Shou University, Kaohsiung, Taiwan. ⁷Department of Pharmacology, School of Medicine, College of Medicine, Kaohsiung Medical University, Kaohsiung, Taiwan. ⁸Division of Pediatric Cardio-Pulmonology, Department of Pediatrics, Kaohsiung Medical University Hospital, Kaohsiung Medical University, Kaohsiung, Taiwan.

⁹Department of Pediatrics, School of Medicine, College of Medicine, Kaohsiung Medical University, Kaohsiung, Taiwan.

Received: 25 August 2023 Accepted: 22 November 2023

Published online: 07 December 2023

References

- Humbert M, Morrell NW, Archer SL, Stenmark KR, MacLean MR, Lang IM, et al. Cellular and molecular pathobiology of pulmonary arterial hypertension. *J Am Coll Cardiol*. 2004;43:135–245.
- Simonneau G, Montani D, Celermajer DS, Denton CP, Gatzoulis MA, Krowka M, et al. Haemodynamic definitions and updated clinical classification of pulmonary hypertension. *Eur Respir J*. 2019;53:1801913.
- Li L, Jick S, Breitenstein S, Hernandez G, Michel A, Vizcaya D. Pulmonary arterial hypertension in the USA: an epidemiological study in a large insured pediatric population. *Pulm Circ*. 2017;7:126–36.
- Wang Q, Chai L, Zhang Q, Wang J, Liu J, Chen H, et al. Induction of GLI1 by miR-27b-3p/FBXW7/KLF5 pathway contributes to pulmonary arterial hypertension. *J Mol Cell Cardiol*. 2022;171:16–29.
- Zhao FY, Xu SL, Zhang CF, Liu J, Zhang Y, Yang J, et al. PDGF mediates pulmonary arterial smooth muscle cell proliferation and migration by regulating NFATc2. *Mol Med Rep*. 2021;23:39.
- Paulin R, Michelakis ED. The metabolic theory of pulmonary arterial hypertension. *Circ Res*. 2014;115:148–64.
- Moench R, Grimmig T, Kannen V, Tripathi S, Faber M, Moll EM, et al. Exclusive inhibition of PI3K/Akt/mTOR signaling is not sufficient to prevent PDGF-mediated effects on glycolysis and proliferation in colorectal cancer. *Oncotarget*. 2016;7:68749–67.
- Xiao Y, Peng H, Hong C, Chen Z, Deng X, Wang A, et al. PDGF promotes the Warburg effect in pulmonary arterial smooth muscle cells via activation of the PI3K/AKT/mTOR/HIF-1 α signaling pathway. *Cell Physiol Biochem*. 2017;42:1603–13.
- Humbert M, Lau EM, Montani D, Jaïs X, Sitbon O, Simonneau G. Advances in therapeutic interventions for patients with pulmonary arterial hypertension. *Circulation*. 2014;130:2189–208.
- Kuo MW, Tsai HH, Wang SH, Chen YY, Yu AL, Yu J. Yulink, predicted from evolutionary analysis, is involved in cardiac function. *J Biomed Sci*. 2021;28:7.
- Bar-Peled L, Chantranupong L, Cherniack AD, Chen WW, Ottina KA, Grabiner BC, et al. A tumor suppressor complex with GAP activity for the rag GTPases that signal amino acid sufficiency to mTORC1. *Science*. 2013;340:1100–6.
- Babicheva A, Makino A, Yuan JX. mTOR signaling in pulmonary vascular disease: pathogenic role and therapeutic target. *Int J Mol Sci*. 2021;22:2144.
- Wu YC, Wang WT, Lee SS, Kuo YR, Wang YC, Yen SJ, et al. Glucagon-like peptide-1 receptor agonist attenuates autophagy to ameliorate pulmonary arterial hypertension through Drp1/NOX- and Atg-5/Atg-7/Beclin-1/LC3 β pathways. *Int J Mol Sci*. 2019;20:3435.
- Wang WT, Lee SS, Wang YC, Lai YW, Kuo YR, Tang Chen YB, et al. Impaired cutaneous T-cell attracting chemokine elevation and adipose-derived stromal cell migration in a high-glucose environment cause poor diabetic wound healing. *Kaohsiung J Med Sci*. 2018;34:539–46.
- Wu YC, Wang WT, Huang LJ, Cheng RY, Kuo YR, Hou MF, et al. Differential response of non-cancerous and malignant breast cancer cells to conditioned medium of adipose tissue-derived stromal cells (ASCs). *Int J Med Sci*. 2019;16:893–901.
- Lee MY, Tsai KB, Hsu JH, Shin SJ, Wu JR, Yeh JL. Liraglutide prevents and reverses monocrotaline-induced pulmonary arterial hypertension by suppressing ET-1 and enhancing eNOS/SGC/PKG pathways. *Sci Rep*. 2016;6:31788.
- Li WX, Chen LP, Sun MY, Li JT, Liu HZ, Zhu W. 3'-Diindolylmethane inhibits migration, invasion and metastasis of hepatocellular carcinoma by suppressing FAK signaling. *Oncotarget*. 2015;6:23776–92.
- Sharma S, Aldred MA. DNA damage and repair in pulmonary arterial hypertension. *Genes (Basel)*. 2020;11:1224.

19. Michelakis ED, Gurtu V, Webster L, Barnes G, Watson G, Howard L, et al. Inhibition of pyruvate dehydrogenase kinase improves pulmonary arterial hypertension in genetically susceptible patients. *Sci Transl Med*. 2017;9: eaao4583.
20. Marsboom G, Wietholt C, Haney CR, Toth PT, Ryan JJ, Morrow E, et al. Lung ¹⁸F-fluorodeoxyglucose positron emission tomography for diagnosis and monitoring of pulmonary arterial hypertension. *Am J Respir Crit Care Med*. 2012;185:670–9.
21. Ohira H, deKemp R, Pena E, Davies RA, Stewart DJ, Chandy G, et al. Shifts in myocardial fatty acid and glucose metabolism in pulmonary arterial hypertension: a potential mechanism for a maladaptive right ventricular response. *Eur Heart J Cardiovasc Imaging*. 2016;17:1424–31.
22. Adhikari N, Basi DL, Carlson M, Mariash A, Hong Z, Lehman U, et al. Increase in GLUT1 in smooth muscle alters vascular contractility and increases inflammation in response to vascular injury. *Arterioscler Thromb Vasc Biol*. 2011;31:86–94.
23. Li L, Xu M, Li X, Lv C, Zhang X, Yu H, et al. Platelet-derived growth factor-β (PDGF-β) induced by hypoxia promotes the survival of pulmonary arterial endothelial cells through the PI3K/Akt/Stat3 pathway. *Cell Physiol Biochem*. 2015;35:441–51.
24. Wang YY, Cheng XD, Jiang H. Effect of atorvastatin on pulmonary arterial hypertension in rats through PI3K/AKT signaling pathway. *Eur Rev Med Pharmacol Sci*. 2019;23:10549–56.
25. Humbert M, Sitbon O, Simonneau G. Treatment of pulmonary arterial hypertension. *N Engl J Med*. 2004;351:1425–36.
26. Bhogal S, Khraisha O, Al Madani M, Treece J, Baumrucker SJ, Paul TK. Sildenafil for pulmonary arterial hypertension. *Am J Ther*. 2019;26:e520–6.
27. Roger I, Milara J, Montero P, Cortijo J. The role of JAK/STAT molecular pathway in vascular remodeling associated with pulmonary hypertension. *Int J Mol Sci*. 2021;22:4980.
28. Sommer N, Ghofrani HA, Pak O, Bonnet S, Provencher S, Sitbon O, et al. Current and future treatments of pulmonary arterial hypertension. *Br J Pharmacol*. 2021;178:6–30.
29. Hsu JH, Li F, Yang SN, Wu BN, Dai ZK, Chen IJ, et al. B-type natriuretic peptide inhibits angiotensin II-induced proliferation and migration of pulmonary arterial smooth muscle cells. *Pediatr Pulmonol*. 2014;49:734–44.
30. Zhang S, Wang J, Qi X, Tao X, Xie W, Wan J, et al. Plasminogen activator inhibitor-2 inhibits pulmonary arterial smooth muscle cell proliferation in pulmonary arterial hypertension via PI3K/Akt and ERK signaling. *Exp Cell Res*. 2021;398: 112392.
31. Wu J, Yu Z, Su D. BMP4 protects rat pulmonary arterial smooth muscle cells from apoptosis by PI3K/AKT/Smad1/5/8 signaling. *Int J Mol Sci*. 2014;15:13738–54.
32. Chen B, Xue J, Meng X, Slutzky JL, Calvert AE, Chicoine LG. Resveratrol prevents hypoxia-induced arginase II expression and proliferation of human pulmonary artery smooth muscle cells via akt-dependent signaling. *Am J Physiol Lung Cell Mol Physiol*. 2014;307:L317–325.
33. Hu Z, Song Q, Ma H, Guo Y, Zhang T, Xie H, et al. TRIM32 inhibits the proliferation and migration of pulmonary artery smooth muscle cells through the inactivation of PI3K/Akt pathway in pulmonary arterial hypertension. *J Bioenerg Biomembr*. 2021;53:309–20.
34. Tang H, Chen J, Fraidenburg DR, Song S, Sysol JR, Drennan AR, et al. Deficiency of Akt1, but not Akt2, attenuates the development of pulmonary hypertension. *Am J Physiol Lung Cell Mol Physiol*. 2015;308:L208–20.
35. Liu X, Liu H, Zeng L, Lv Y. BRCA1 overexpression attenuates breast cancer cell growth and migration by regulating the pyruvate kinase M2-mediated Warburg effect via the PI3K/AKT signaling pathway. *PeerJ*. 2022;10: e14052.
36. Long WB, Pu X, Tang Y, Li M, Liu Y, She Q, et al. Arginine ADP-ribosyltransferase 1 regulates glycolysis in colorectal cancer via the PI3K/AKT/HIF1α pathway. *Curr Med Sci*. 2022;42:733–41.
37. Sun Z, Tan Z, Peng C, Yi W. HK2 is associated with the Warburg effect and proliferation in liver cancer: targets for effective therapy with glycyrrhizin. *Mol Med Rep*. 2021;23:343.

Publisher's Note

Springer Nature remains neutral with regard to jurisdictional claims in published maps and institutional affiliations.

Ready to submit your research? Choose BMC and benefit from:

- fast, convenient online submission
- thorough peer review by experienced researchers in your field
- rapid publication on acceptance
- support for research data, including large and complex data types
- gold Open Access which fosters wider collaboration and increased citations
- maximum visibility for your research: over 100M website views per year

At BMC, research is always in progress.

Learn more biomedcentral.com/submissions

